Elizabeth Jesse
Embry Riddle Aeronautical University
Prescott, Az

Final Report

Introduction

Three distinctive projects were pursued this summer. The main project involved using the Atomic force Microscope (AFM), first in scanning mode for surface scanning and bond imaging, then indenting materials to determine Young's Modulus. The second project used an ellipsometer to determine layer thicknesses, most importantly thermally grown oxide layer thicknesses on silicon samples. The third main project was setting up an Optical Spectrum Analyzer to determine characteristics of various lasers.

Background

AFM Imaging

AFMs use nano-scale probes on cantilevers to scan surfaces to accuracies on the order of tens of angstroms. There are several methods of doing this, the main two used in this research were 'contact mode' and 'tapping mode'. In general, a laser is reflected off the tip and the tip location is read on a split photo diode while the cantilever base location is determined from the voltage applied to the PZTs which control tip movement.

In contact mode, a tip is dragged across the surface. A feedback loop maintains a constant tip deflection and the height of the PZT determines the height of the surface for that data point. A map of these points is created to give a surface map with resolutions up to <100 A, depending on the tip. The tip used here was a V-shaped silicon nitride tip with a radius of curvature from 20-60 nm.

For some materials, in this case silica, contact mode does not work well and creates blurred images with a lot of streaking from debris being dragged across the surface. For these samples 'tapping mode' was used. Tapping mode is much less invasive than contact mode and is less likely to cause damage, especially when using a diamond tip. The tip used for this mode is a silicon tip with a radius of curvature of 5-10nm and a resonance frequency of 200-400 kHz. Tapping mode oscillates the tip near its resonance frequency. When the tip comes into contact with the surface it taps the surface lightly, reducing the amplitude of oscillation. A feedback circuit maintains constant amplitude and the height of the surface can be determined and mapped.

These surface maps were used to look at hydroxide catalysis bonds of silica to silica and silicon to silicon. The samples looked at were thin slices through bonded disks and the surfaces of bonds which had been sheared apart. The purpose of these was to look at the thicknesses of the bonds in the slices and to determine if any characteristics of the bonds could be determined from the surfaces of the sheared samples.

AFM Indenting

AFMs have another mode called ‘indenting’. In this mode, a steal cantilever with a diamond tip is pressed into the surface at a variety of rates and depths. For each dent, a force plot is made of cantilever deflection versus Z-displacement of the base. For these curves, a calibration on a hard surface is required to determine the deflection of the cantilever per amount of force, which can then be subtracted from the force curve to give the force per depth curve for the indented material. Ideally an infinitely hard surface would be used to obtain the calibration curve; this is not possible so sapphire was used as it has hardness near that of diamond. After indentation, a tapping mode scan is used to map the indent.

These indents can be used to determine the hardness and young’s modulus of materials. The materials used in this research were silica, copper, and steal. The purpose of this was to calibrate the indentation procedures on known materials. Eventually, this method can be used to determine the young’s modulus of surface layers and thin films, which may be different from the bulk material. An application of this are the thin film stacks used in LIGO.

Ellipsometry

Ellipsometry is the study of a material from the polarization state change induced by the reflection of a coherent beam off of the material. A basic setup can be seen below (Figure 1). This method is especially useful for samples consisting of one or more layers of thin films and can determine thickness, the complex index of refraction, birefringence, and other optical properties for each layer.

As light of a known polarization interacts with a surface, some will reflect, some will be transmitted, and the rest will absorbed. The relative amplitudes of each depend on the material properties and incident angle. In ellipsometry, we generally look at the reflected beam only and investigate the difference between the effect of the sample on s and p polarized light.

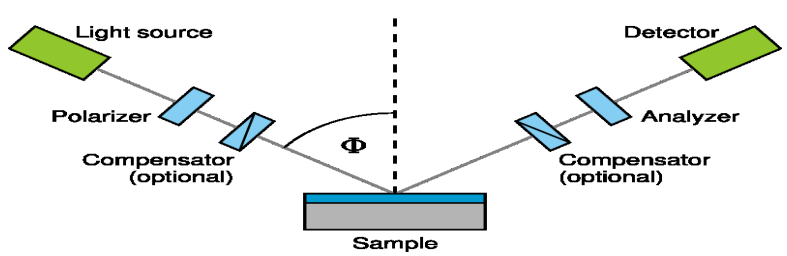

Figure 1: Basic Setup of an Ellipsometer

A measurement at a given angle of incidence and wavelength of light will provide two values, $\tan\Psi$ and $\cos\Delta$, defined as

$$\tan\Psi = \frac{|r_p|}{|r_s|}$$

$$\Delta = \delta_1 - \delta_2$$

where and r_p and r_s are the complex reflection coefficients of the material, δ_1 is the phase difference between the s and p polarizations before reflection, and δ_2 is the phase difference afterwards. From these we can construct the ratio of complex reflection coefficients, ρ, by

$$\rho = \frac{r_p}{r_s} = \tan\Psi e^{i\Delta}$$

The ratio, ρ, of the complex reflection coefficients can be modeled for a given layer stack. This ratio depends on the number of layers, thickness, wavelength, complex index of refraction, etc. To fit to a function that has multiple variables, we need at least one data point per variable. To obtain a large number of data points we use spectroscopic ellipsometry and use a material model to obtain the complex indices of refraction at different wavelengths.

Spectroscopic ellipsometry uses the same principles; however it measures over a range of wavelengths, making Ψ and Δ functions of wavelength. The index of refraction model is required to fit the desired variables. This method gives enough information to fully determine the parameters of the sample.

The main layer structures studied in this research were oxide thicknesses on silicon. These layers will be bonded together using hydroxide catalysis bonding methods, the same as will be used in Advance LIGO. Accurate oxide layer thicknesses are important to modeling the baking process used to grow the layers. So far several methods for measuring this thickness have been used, but with a wide variety of results. This method will be compared to the others to determine the value which will be used in the models. Other samples were also measured, one such was a 15 pair Halfnia silica stack, however this will be continued at a later date.

Optical Spectrum Analyzer

The Optical Spectrum Analyzer utilizes a confocal Fabry-Perot cavity to determine the spectrum of an input beam. A Fabry-Perot cavity uses two highly reflective mirrors to create a cavity in which incident light is reflected multiple times. The light interferes with itself such that if the optical path length between the two mirrors is an integer number of wavelengths it builds constructively until a significant portion leaks out the end mirror. If the optical path length is at any other length the light levels in the cavity only allow a very small amount of light to seep out.

The Spectrum Analyzer uses a PZT to move one of the mirrors and change the optical path length of the cavity. As the PZT changes the length, the cavity will resonate at different lengths. The distance between resonates is one quarter wavelength. This is known as the Free Spectral Range, FSR. If the distance the PZT moves is known and the FSR is know, this method can be used to determine the wavelength of incident light.

Data and Analysis

AFM scanning

For each slice, the sample was placed loosely on the table (no drift was present). Each end was scanned and the entire length of the bond was optically examined, if any anomalies were present they were also scanned. The scan size was usually 50-80 um with a resolution of 512 points/line and 512 lines/scan.

In most samples there was a noticeable difference in bond thickness between the two ends. The extent of this horizontal wedging was in the range of 1-3 times thicker at one end than the other. A series of scans showed that this was a gradual increase from one end to the other. Also, this seems to be thickness dependant, the thicker the bond the larger the ratio of one end to the other, however there was not enough information to verify this. Due to this wedging, it was not possible to compare the bond thicknesses to other measurement methods; however the thicker oxide layers did correspond to thicker bond layers, as expected.

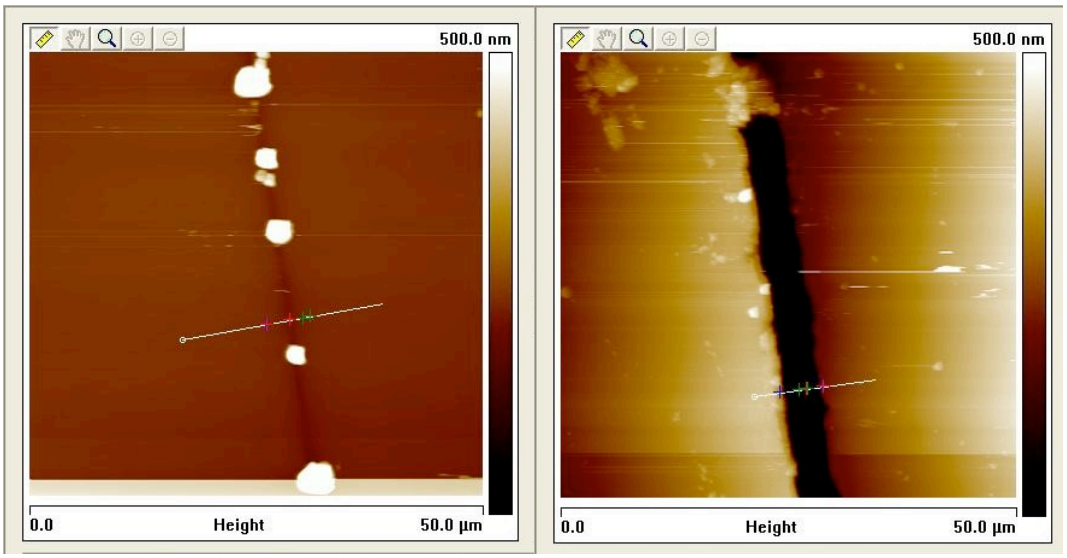

Figure 2: Comparison of the two ends of a single bond.
Both on 50um scans where height is denoted by color.

Another anomaly which occurred in about half of the slices was a vertical wedging. In each case, the vertical wedging occurred in the end with the thicker

bond. The height differences were on the order of 0-3um. This is an important property because each of these samples goes through a polishing process prior to being scanned which should cause the sides to be flat within $\lambda/6$. During this process, each of the slices is mounted in wax to hold them in place without damaging the surface. Because each of the sides is flat, without rounded corners, this suggests that this wedging occurs during unmounting or in the late stages of polishing.

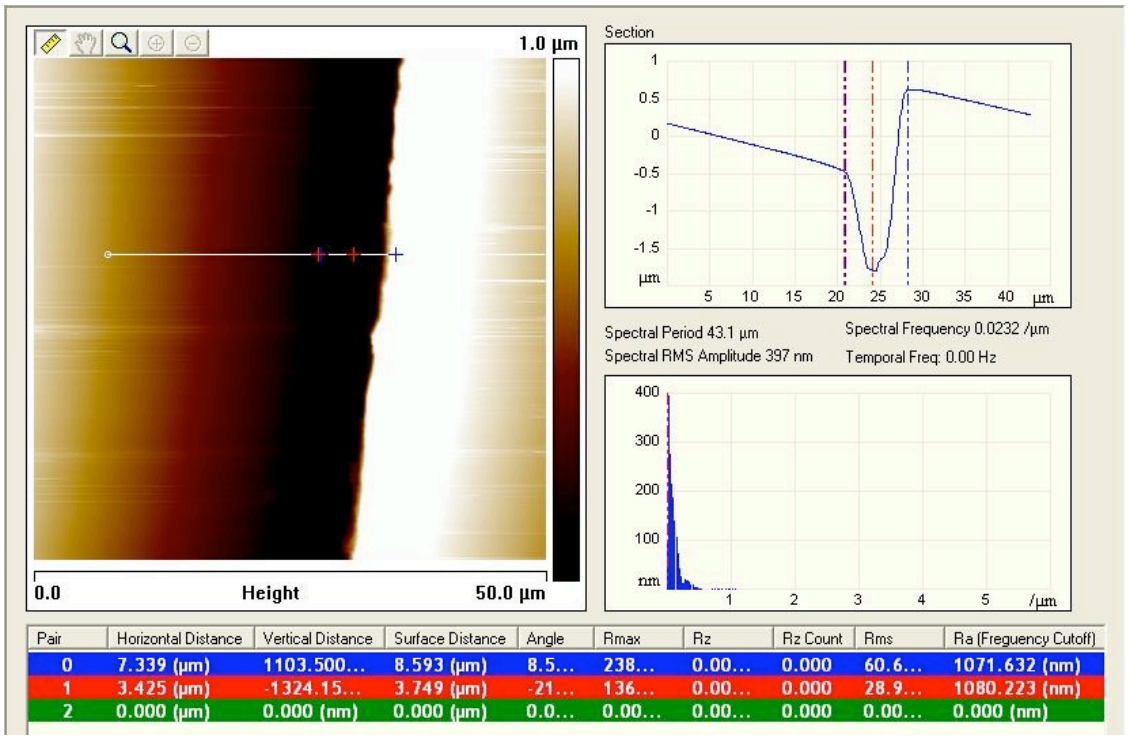

Figure 3: Surface height map. Slice along line shows vertical wedging.

One of the silicon samples was found broken in the box. The bonded surface was scanned and a definite layer pattern was found that corresponded to the known oxide and bond layer thicknesses. This layer pattern took on a distinctive flower pattern (see Figure 4). A second sample, silica this time, was purposefully broken for comparison, however it did not display the same pattern and distinctive layers were not apparent. Due to the way the first sample was broken, it suggests that this bond was weakened during the bonding process in a way that resulted in the distinctive pattern. The layer structure visible in the silicon sample prompted looking at the sheared samples to determine if it could be found in controlled silicon breaks.

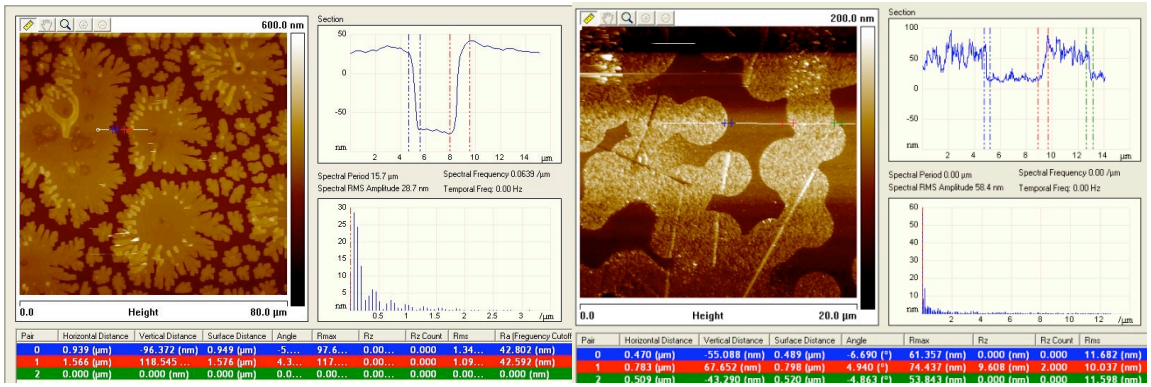

Figure 4: Bond surface maps. Left: flower patter on silicon break. Right: bubble pattern on silica break.

Each shear sample was scanned and two common layer structures were found. The first was a layer that was 150-350 nm thick, and was consistent within 5 nm across the entire sample. The second layer pattern, which was only found in 3 of the 8 samples, was 3-5 nm thick. The consistency of these layers suggests that it is indicative of some property of the samples; however they did not correspond with known layer thicknesses.

AFM Indenting

The first step in calculating the young's modulus, E, is to find the sensitivity of the cantilever. The cantilever will bend as more force is applied which must be subtracted off of the force curves. The sensitivity calibrations were all taken on sapphire as it was the hardest surface available. The slope of the curve in V/nm is the sensitivity (see Figure 5). Because of slight variations between indents, arrays of 9 or more calibration indents were taken each time and averaged to find the sensitivity used in subsequent indents. To maintain accuracy, the laser and cantilever positions were maintained until all indentations were complete.

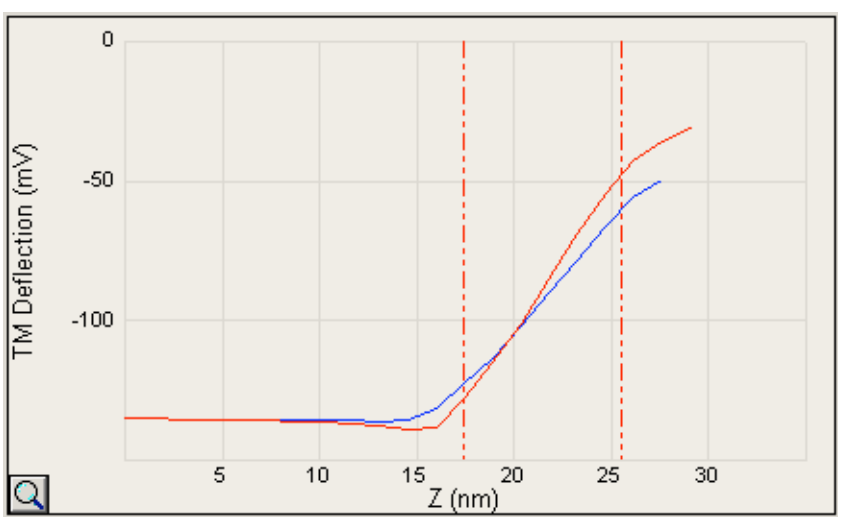

Figure 5: Sample calibration curve on sapphire

Next, force curves for each material were obtained. Again, on each sample an array of indents was made for statistical purposes. The force of each indent was set according to the material. Once the curve is obtained, the area is scanned in extremely high resolution using tapping mode. The sensitivity of the cantilever is then subtracted from the force curve to give a true force vs. displacement plot.

From the true force plot (after subtracting the sensitivity) the elastic unloading stiffness can be found as the slope of the steepest portion of the curve. Stiffness is defined as the resistance of an elastic body to deflection or deformation by an applied force. This is measured on the retract curve, not the approach curve, because the approach curve includes both plastic and elastic deformation, the retract curve only has elastic. Some methods include indenting the same position several times to ensure that only elastic deformation is taken into account, however, due to drift this was not possible in this case.

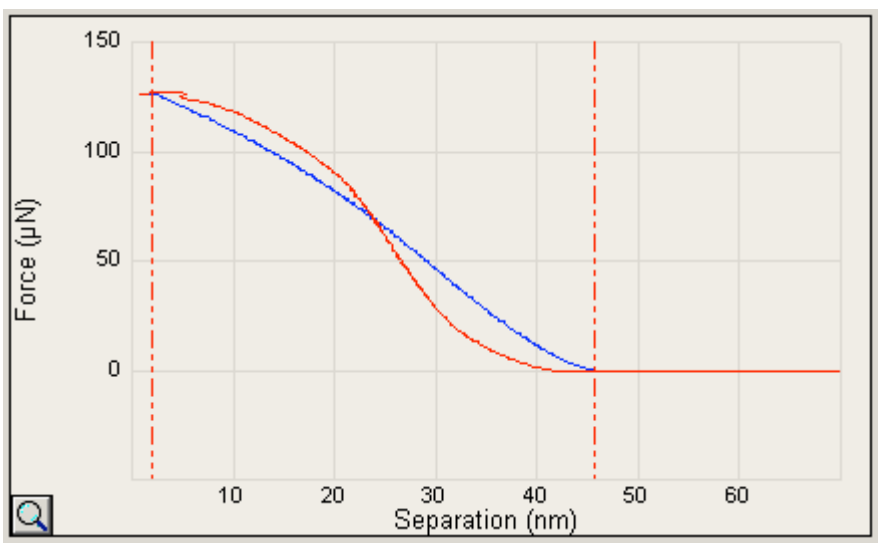

Figure 6: Sample force plot (after subtracting sensitivity) on silica.

The maximum depth of penetrations can be found from the depth of the approach curve. The depth of contact, which is the depth less sink in, must then be calculated (This must be done because the contact area is the surface area of the indenter touching the surface, not just the c/s of the indent, and the indenter does not touch as deeply as maximum depth due to sink in). This depth is:

$$h_c = h_{\max} - \varepsilon \frac{P_{\max}}{S}$$

Where $P_{\max}$ is the maximum force, S is the contact stiffness, $h_{\max}$ is the maximum depth of penetration of the tip and ε is a constant dependant on tip geometry. For a triangular pyramid $\varepsilon = 0.75$ is acceptable (Oliver and Pharr, 2005).

The area of the indent is the area of the indenter touching the material. This is calculated using the equation for the area of a pyramid less the base:

$$A = \frac{\sqrt{2}}{2} * h_c * (s_1 + s_2 + s_3)$$

The side lengths, s, are measured using the scans of the surface after indenting.

Next the reduced Young's modulus can be calculated using:

$$E_r = \frac{S\sqrt{\pi}}{2\beta\sqrt{A}}$$

where β is factor used to account for axial asymmetry in pyramidal indenters and is taken to be 1.05 (Oliver and Pharr, 2005). The reduced Young's Modulus is the result of combining the material indented and the indenter itself. To get the measured Young's Modulus, the following correction was used:

$$\frac{1}{E_r} = \frac{(1-\upsilon^2)}{E} + \frac{(1-\upsilon_i^2)}{E_i}$$

where subscript i denotes the indenter values.

Following these steps, the values in Table 1 were found.

Table 1: Young's Modulus Measurements

Material	Measured E [Gpa]	Accepted E [Gpa]
Silica	16-44	78
Copper	10-59	110-128
Steel	65	190-210
Gold	38	78
Aluminum	--	69

The measured values are distinctively lower than the accepted values. The main reason for this is the area measurement. The tip was put into the SEM and it was determined that there was a large piece of metal stuck to the tip. The size of the piece was on the order of several um and should greatly affect the indentations, whose maximum depths are on the order of 100 nm. Several attempts were made to remove this piece including indenting deeply into and dragging across a soft gold plate, blowing lightly with compressed air, and a minute in an ultrasonic bath, however these efforts were not able to remove the piece completely.

Aside from the piece on the tip, there is still some confusion on how to find the area. The method employed here assumes a perfect pyramid tip with a correction factor incorporated later. This requires finding the side lengths of the indent; however, where to measure that is unclear. Due to sink in, pile up and poorly defined edges, where these lengths should be measured is up to interpretation.

Ellipsometry

The ellipsometer utilizes software that comes with the machine to build models. The difficulty remains to build an accurate model of the system. Most layers in the fitting program do not take into account absorption or roughness. To calculate these, there are several correcting layers that can be added to the model. Also, thin layers such as natural oxide layers, may be present. These are difficult to model because they are not well known.

The main use was to determine the thickness of a single oxide layer on a silicon substrate. Most of the data fit the models well, however there was an anomaly around 1100nm (see Figure 7), which was unable to be explained by absorbing layers, roughness layers or by changing the formula used to simulate the layer. Even with this anomaly, the results, seen below, were within +/- 1 nm whether or not the full range or a partial range of wavelengths were used.

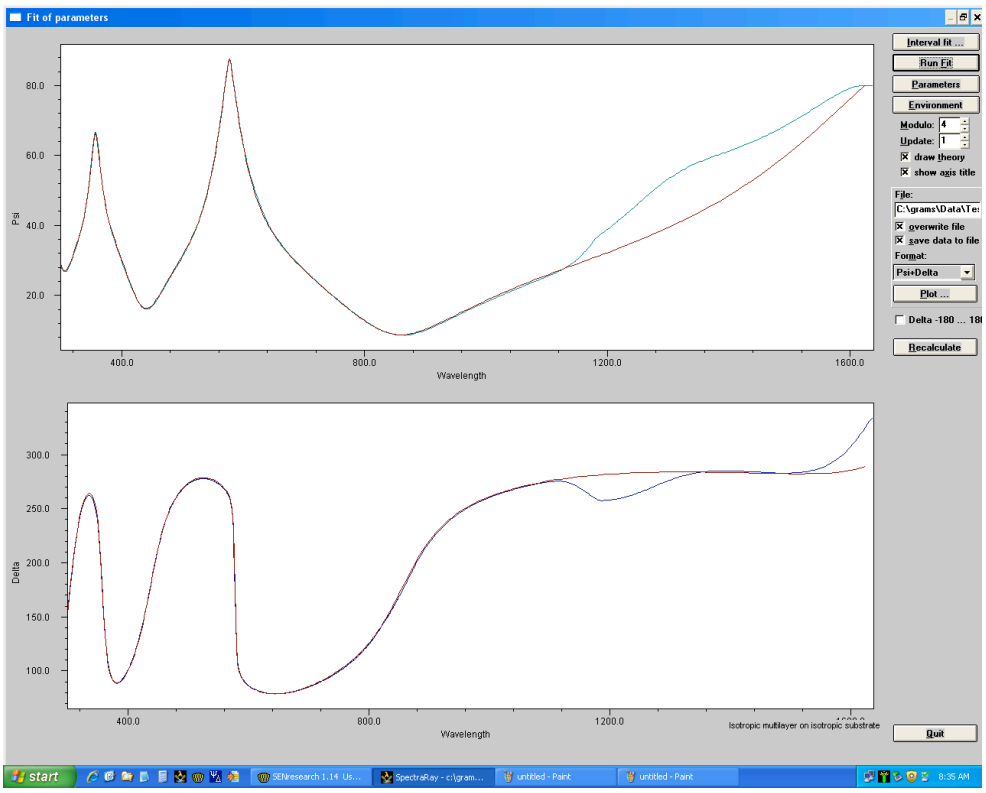

Figure 7: 200nm oxide layer fit with anomaly at 1100nm.

Table 2: Oxide Layer Thicknesses

Oxidation Regime	**ZYGO**	**WYKO**	**Talisurf**	**SEM**	**Ellipsometry**
50 nm, 1000 C, wet	-	-	40	40	42
100 nm, 1000 C, wet	-	-	69	68	59*
200 nm, 1000 C, wet	45	30	90	83	91

100 nm, 920 C, dry	100	100	250	250	253
50 nm, 1000 C, dry	40	56	110	-	104
100 nm, 1000 C, dry	100	100	200	-	205
200 nm, 1000 C, dry	190	200	350	200	386

Several other tests were performed on 15 pair layer stacks of Halfnia or Tantala and silica. These tests came up with very accurate layer thicknesses compared to the quoted values. Tantala was more difficult to analyze and the data sets were much noisier, making lower layers not as affected by the fit. Overall, this was verified as a method for determining multi-layer systems.

Cavity

The cavity will resonate if the there are an integral number of wavelengths in the optical path length.

$$nd\cos\Theta = \frac{m\lambda}{4}$$

When the beam is perpendicular to the mirrors the cosine term is 1. If the path length changes, the equation becomes:

$$nd + x = \frac{(m+1)\lambda}{4}$$

Where x is the length the cavity must change for there to be an optical path length difference of one wavelength (m+1). The physical distance that the PZT moves can be calibrated to a known wavelength.

$$x = \frac{\lambda}{4} * \frac{ramp[ms]}{peaktopeak[ms]}$$

Where ramp [ms] is the time interval, measured on the oscilloscope, that the PZT takes to move its full range and peaktopeak [ms] is the time interval it take s the PZT to move through the FSR

$$FSR = \frac{\lambda}{4}$$

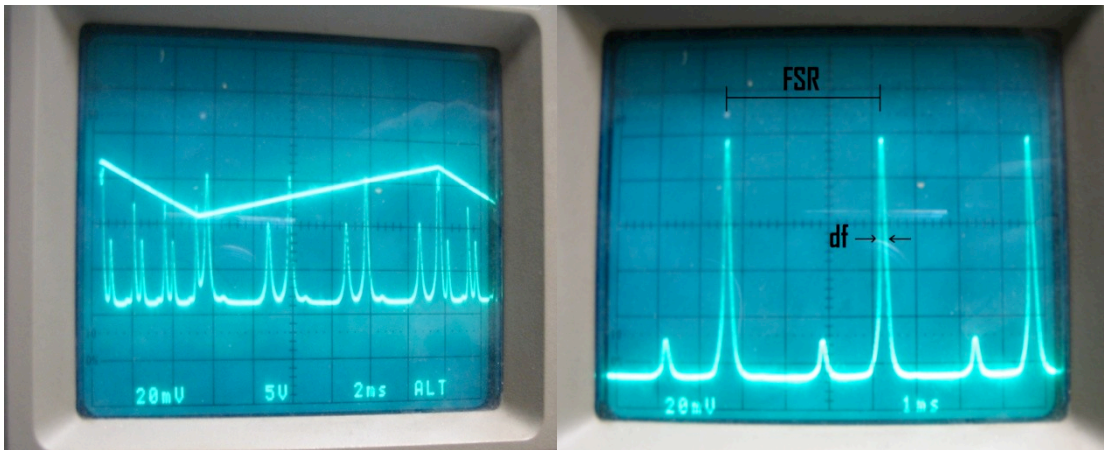

Figure 8: Output of spectrum analyzer. Left: PZT length and light output. Right: Output after warm-up time

By using a known laser frequency, such as a HeNe laser at 632.8 nm, to calibrate x, we can determine the wavelength of an unknown laser. We can also determine the wavelengths of any secondary laser modes present.

Using this method, the wavelength of a green laser was found to be 530.182nm +/- 10.6nm. The wavelength printed on the laser was 532nm; this was well within error. The main source of error came from the resolution of the oscilloscope. Also, the secondary laser modes that were present shifted continuously until the laser heated up. This was confirmed by externally heating the laser to reduce warm up time.

The finesse of the cavity was also measured. The finesse is the ratio of FSR to the cavity linewidth and is a 'goodness' measurement of the cavity. The higher the finesse, the more times the light will, on average, bounce back and forth in the cavity.

$$\Delta f = \frac{FSR}{finess}$$

The finesse for the cavity was measured to be 36. The cavity was rated to have a finesse >200. While investigating this, we took the cavity apart and discovered one of the mirrors was dirty. To clean it, we wiped it twice with methanol at which point the coating began to come off, so we poured the methanol over the mirror instead. This caused large portions of the reflective coating to come off. It was determined that the cause of this was that they were 'soft coated' metal mirrors and should not have been cleaned at all. A new set of mirrors was ordered, however further use of the cavity is pending their arrival.

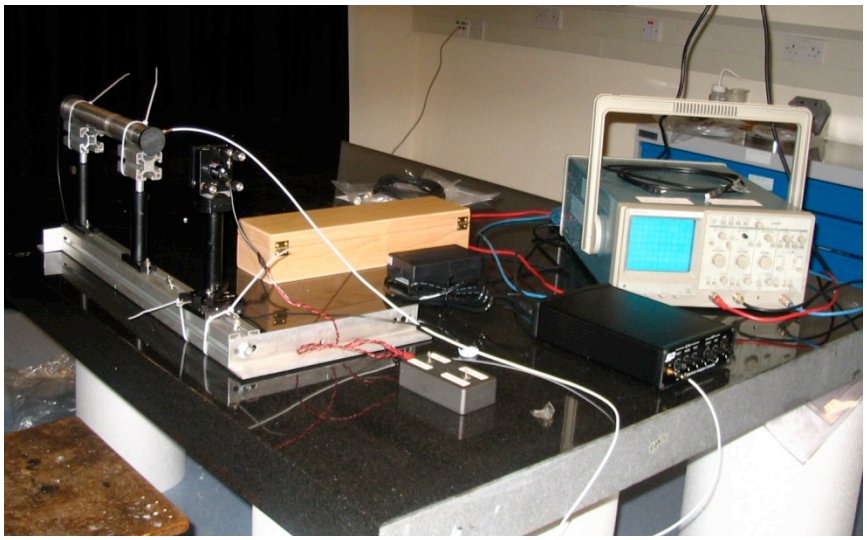

Figure 9: Spectrum analyzer setup

Conclusions

AFM Imaging

The horizontal wedging is a known problem with the bonds which is currently being looked into. The AFM has proven to be one of the most useful tools to see this effect. The vertical wedging is an unknown problem which may be caused by the polishing process. During polishing, the samples are mounted in wax which may not be supporting the sample well enough to reduce the stresses in the bond. The polishing process itself may also be applying forces to high for the bonds to withstand. Future research will look at the bonds before, during each step, and after polishing and before and after unmounting in the wax to determine where this wedging is occurring. This may lead to a change in polishing procedures.

In the sheared samples, the lack of consistency in visible surface area and the incompatibility of the visible layer thicknesses to known layer thicknesses, suggests that this is not a viable means for determining bond thicknesses. The unique patterns that were seen on the accidentally broken bond may be compared to known fracture patterns at a later date to determine what the cause of the bond weakness was.

AFM Indents

The results were consistently low for all of the materials examined in this research. The main cause of this appears to be the area estimation. First, the tip has to be cleaned or replaced to get an accurate measurement, especially if the model used assumes a perfect pyramid. Second, a consistent method of measuring the area must be developed.

There are three methods most likely to lead to good results. The first is to find a consistent way to measure the side lengths of the indent and finding the correct correction to translate the plastically deformed area to total area. This method is

desirable because it would give a measured value based on the information already provided. The issues with this method are that the amount of elastic deformation per plastic deformation will change for each material and may not be linear with indent depth for all materials.

The second method is to take a known sample, such as silica, and create an area model based solely on the contact depth of penetration. This would reduce the amount of uncertainty in how to find the area and would be consistent between materials. However, this method relies on knowing a certain material very well (while silica is well know, the water absorbed in the surface layer affects the measurements, etc…) , and would require a large amount of data to get a good model due to the large variation in data. Also, this method is dependent on having the same angle of incidence for all indents, which may be a problem as the cantilever was visibly bent in the SEM images and is likely to bend more over its lifetime.

The final method is to image the tip very accurately in an SEM and create an area model based on angle of incidence and contact depth. This would be the most accurate and preferable method. However, because the tip is made of diamond, it is difficult to image accurately in an SEM. There are several methods to get around this, however most, such as a thin coating of spattered gold, would be destructive to the indenter accuracy.

Once these issues are addressed, other smaller issues can be corrected. One such is comparing the calibration on the sapphire to a calibration on diamond to see it that has any affect. The sensitivities found on this AFM were much lower than the calibration that came with the tip. This should be a result of different PZT sensitivities, however it is an issue that should be looked into and verified that it is not a problem. A second minor correction is [beta]. It has so far been assumed to be 1.05, however, further research will be required to find out if this is the true value as other research has shown values from 0.95 to 1.2. Several fit this factor to silica test.

Ellipsometry

The values from the ellipsometer tests verified that the Talisurf and SEM values for oxide layers are correct. At the same time, these tests showed the viability of using this method to find layer thicknesses with relative ease and accuracy. While determining what parameters are required and most important for fitting on the first sample with a given layer structure can be difficult and time consuming, once these variable are determined, subsequent samples are easily measured and fit with accuracy.

The ellipsometer was also shown to be able to handle multi-layer stacks. This method is limited to well known samples, however. If starting values more than about 10% off from true values were used, the fit did not converge. This can be partially remedied by hand fitting the data more extensively after initial fitting, however this is a difficult and time consuming task. Also, if there was an unknown layer the model would not fit well, no matter the amount of adjustment.

Overall, this will be a useful and accurate tool for a variety of uses. There are also many useful functions, such as the $dn/d\lambda$ generator. The one thing that was

found lacking was the error estimate. The cited errors were incredibly small and not useful. One way around this is to take several measurements at different places around the sample and determine error based on the variation.

Cavity

The measurements of the green laser were well within error of what was cited on the laser. The sidebands that were visible seemed to be entirely heat related as they disappeared nearly entirely after about an hour of being on. The accuracy could be greatly increased if the finesse were increased.

Once the new mirrors come in, the cavity is now setup such that new lasers are easily aligned and measured. From these measurements the wavelength can be found and other laser modes can been seen and measured. Settling time for the lasers can also be determined. This will be useful for experiments where exact and steady wavelengths are required.

References

1. (1993). Ellipsometers. In *Encyclopedia of Applied Physics* (Vol. 6). VCH Publishers, Inc..
2. Guo, Akhremitchev. "Investigation of Mechanical Properties of Insulin Crystals by Atomic Force Microscopy." Langmuir (2008): 880-887
3. Oliver, Pharr. "Measurement of hardness and elastic modulus by instrumented indentation: Advances in understanding and refinements to methodology." Journal of Materials Research 19(2004): 3-20.
4. Thompkins, H, & McGahan, W (1999). *Spectroscopic Ellipsometry and Reflectometry: A User's Guide*.New York: John Wiley & Sons, Inc..
5. van Veggel, "Hydroxide Catalysis Bonding of Silicon to Silicon." (2007):